

KAWASAKI STEEL TECHNICAL REPORT

No.42 ( May 2000 )

---

Magnetic Properties of High Permeability Iron Powder "KIP MG270H" for Line Filter Cores

Yukiko Ozaki, Masashi Fujinaga

---

Synopsis :

The initial permeability of reduced iron powder cores has been investigated in relation to the effects of material characteristics dependence, impurity concentration, grain size and residual strain introduced during the compacting process. The reduction of impurities (O, C, P and S) and coarsening of grains have been found effective for improving the permeability. Transmission electron microscope observation around the grain boundaries of an iron particle revealed that nonmagnetic inclusions are formed along the grain boundaries with sizes comparable to the domain wall thickness of pure iron. This fact suggests that the grain boundaries act as the sites of strong pinning of the domain wall displacement. On the basis of these findings, Kawasaki Steel has developed a new reduced iron powder "KIP MG270H", realizing permeability higher than the conventional materials up to several hundreds Hertz. This material is applicable to line noise filter cores.

(c)JFE Steel Corporation, 2003

**The body can be viewed from the next page.**

# Magnetic Properties of High Permeability Iron Powder “KIP MG270H” for Line Filter Cores\*



Yukiko Ozaki  
Dr. Sci., Senior  
Researcher, Iron  
Powder & Magnetic  
Materials Lab.,  
Technical Res. Labs.



Masashi Fujinaga  
Staff Manager,  
Iron Powder &  
Welding Materials  
Technology Sec., Iron  
Powder & Welding  
Materials Dept.,  
Chiba Works

## 1 Introduction

With controls over harmonic interference and electromagnetic interference becoming enhanced, an increasing number of noise filters have been used in order to remove the noise produced near the power sources of various kinds of electronic equipment. Sintered ferrite cores are used in high-frequency applications and ferrous metal powder cores of high saturation flux density are used in applications requiring DC bias magnetic flux density in medium- and low-frequency bands. Dust cores made of pure iron have been field proven as good-quality noise filters and have the highest production among ferrous metal powder cores.

Electrolytic iron powder and reduced iron powder are used most frequently as the materials for pure-iron dust cores. Although electrolytic iron powder has relatively high permeability, it is expensive to produce. Reduced iron powder has lower permeability, and fields in which reduced iron powder is used have been limited although it is less expensive than electrolytic iron powder.

Research on the magnetic properties of iron powder has been carried out mainly in relation to the atomized iron powder used in magnetic clutches, etc., and there have been reported on the relationship between the grain

## Synopsis:

*The initial permeability of reduced iron powder cores has been investigated in relation to the effects of material characteristics dependence, impurity concentration, grain size and residual strain introduced during the compacting process. The reduction of impurities (O, C, P and S) and coarsening of grains have been found effective for improving the permeability. Transmission electron microscope observation around the grain boundaries of an iron particle revealed that nonmagnetic inclusions are formed along the grain boundaries with sizes comparable to the domain wall thickness of pure iron. This fact suggests that the grain boundaries act as the sites of strong pinning of the domain wall displacement. On the basis of these findings, Kawasaki Steel has developed a new reduced iron powder “KIP MG270H”, realizing permeability higher than the conventional materials up to several hundreds Hertz. This material is applicable to line noise filter cores.*

size and compressibility of iron powder and flux density<sup>1,2)</sup>, the relationship between the shape, impurity concentration and the microstructure of iron powder and flux density or iron loss<sup>3-5)</sup>, etc. However, few studies of reduced iron powder have been done. In the present study, therefore, in order to improve permeability and reduce dispersion of permeability, an analysis was conducted of the relationship between the characteristics of powder, impurity concentration, inclusions, microstructure of powder and strain introduced during compacting, and the initial permeability of iron powder cores. This report describes the results of this analysis and the magnetic properties of a high-permeability reduced iron powder, KIP MG270H, developed on the basis of the knowledge obtained through the analysis.

## 2 Concept of Improvement of Initial Permeability of Powder Core

### 2.1 Expression of Magnetic Properties of Powder Core

Cores made of ferrous metal powder are divided into

\* Originally published in *Kawasaki Steel Giho*, 31(1999)2, 130-134

powder cores, in which powders are pressed with lubricant and binder, and sintered cores. The former cores are used in higher frequency bands than the latter and their main applications are in noise filters used to absorb the noise near the power sources of electronic equipment.

The magnetic properties of powder cores are evaluated mainly by the complex initial permeability ( $\mu_i'/\mu_0$ ,  $\mu_i''/\mu_0$ ) or initial permeability ( $\mu_i/\mu_0 = (\mu_i'^2 + \mu_i''^2)^{1/2}/\mu_0$ ) and the iron loss per unit volume  $P_{cv} = \pi f H_m^2 \mu_i''$ . In this equation,  $f$  denotes the frequency measured,  $H_m$  the maximum magnetic field intensity applied, and  $\mu_0$  the permeability in a vacuum. Values of initial permeability are often used in analyses in which the initial permeability in ranges of sufficiently low frequency with a negligible effect of eddy currents is regarded as the DC initial permeability  $\mu_{i,DC}/\mu_0$ . According to Ollendorf, the application of Lorentz's theory makes it possible to express  $\mu_{i,DC}/\mu_0$  by the following equation<sup>6)</sup>.

$$\mu_{i,DC}/\mu_0 = \eta(\mu_i - \mu_0) / \{N(1 - \eta)(\mu_i - \mu_0) + \mu_0\} \cdots (1)$$

Where  $\eta$  is the packing fraction,  $N$  is the effective demagnetization coefficient of particles in the core, and  $\mu_i$  is the intrinsic permeability to the core material. According to this equation, it is apparent that  $\mu_{i,DC}/\mu_0$  is determined by the density of magnetic material per unit volume (property as an aggregate of particles), the demagnetization coefficient dependent on the shape of particles (property dependent on the appearance of particles) and the permeability of the particle material (property dependent on the internal structure of particles). Therefore, these governing factors are important for gaining an understanding of the level of the initial permeability of powder cores.

## 2.2 Factors Affecting Initial Permeability of Powder Core

To improve the magnetic properties of powder cores, it is important to quantitatively relate the magnetic properties to the basic physical properties of a material on the basis of a theoretical model. Takajo et al. succeeded in quantitatively explaining the relationship between various properties of ferrous powders and green compacts and the initial permeability and iron loss, and this result provides an effective guideline for the material design of powder cores<sup>7,8)</sup>. The physical properties of each powder considered in this analysis are the shape and size of particles and the oxidation condition of surfaces. These properties are obtained, so to speak, when particles are observed from the outside. As is apparent from Eq. (1), however,  $\mu_i$ , which is intrinsic to the particle material, is one of the factors affecting the initial permeability and it is necessary to conduct an investigation by taking into consideration the internal structure of particles that affects the migration of domain walls, such as the residual strain introduced during the iron powder manufacturing process and the compaction of green compacts, grain boundaries, precipitates and the existence of a sec-

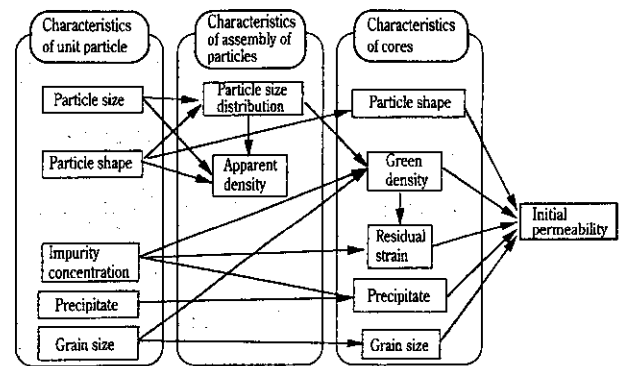


Fig. 1 Mechanisms of controlling the initial permeability of iron powder cores

Table 1 Characteristics of iron powders

Sample	Apparent density (Mg/m <sup>3</sup> )	Chemical composition (mass%)				Green density* (Mg/m <sup>3</sup> )
		O	C	P	S	
A	2.67	0.291	0.003	0.010	0.014	6.76
B	2.62	0.288	0.002	0.008	0.011	6.78
C	2.65	0.316	0.004	0.008	0.009	6.76
D	2.67	0.310	0.002	0.005	0.015	6.80
E	2.69	0.303	0.002	0.006	0.011	6.82
F	2.68	0.310	0.002	0.012	0.011	6.78
G	2.67	0.309	0.003	0.007	0.012	6.80
H	2.65	0.296	0.001	0.006	0.013	6.80
I	2.74	0.334	0.001	0.006	0.012	6.86
G	2.66	0.320	0.004	0.006	0.013	6.87
K	2.68	0.252	0.001	0.011	0.003	6.80
L	2.67	0.356	0.001	0.009	0.003	6.83

\*Compacting pressure: 490 MPa

ond phase. From this point of view, the relationship between the initial permeability and the material properties, depicted in Fig. 1, was verified in this study. This diagram was prepared on the basis of the correlation diagram between the powder characteristics and the magnetic properties of iron powder cores.

## 3 Analysis of Factors Affecting Initial Permeability of an Iron Powder Core

### 3.1 Method of experiment

#### 3.1.1 Raw materials used

Reduced iron powders with different characteristics were used as samples. Table 1 shows the apparent densities, green densities (compacting pressure: 490 MPa) and chemical compositions of these iron powders.

#### 3.1.2 Preparation of test pieces

Test pieces of hexahedral and ring shapes were obtained by mixing 1 mass% zinc stearate (made by NOF Corp.) with powder and compacting the mixture at

Table 2 Initial permeability at 10 kHz and integrated width on the surface of green compacts of iron powders

Sample	Initial permeability $\mu_{i,10k}/\mu_0$	Integrated width ( $^{\circ}$ )
A	69.0	0.349
B	69.7	0.349
C	70.3	0.358
D	70.7	0.350
E	71.1	0.353
F	72.1	0.354
G	72.3	0.371
H	72.3	0.365
I	73.0	0.364
J	73.2	0.346
K	74.8	0.338
L	77.7	0.350

a compacting pressure of 490 MPa.

The hexahedral test pieces (35 mm in length, 10 mm in width, 5 mm in height) were used to observe the structure of particles in green compacts and to conduct X-ray diffraction measurement, and the ring test pieces (38 mm in outside diameter, 25 mm in inside diameter, 6.2 mm in height) were used to measure the complex initial permeability.

### 3.1.3 Measurement

A wire of 0.6 mm in diameter was uniformly wound 11 turns around a ring-shaped iron powder core and the complex impedance was measured in the range of 10 kHz to 1 MHz by means of an impedance meter (Type 4824 A made by Hewlett-Packard Japan Co., Ltd.) and converted to the complex initial permeability. The values of initial permeability were represented by the value at 10 kHz,  $\mu_{i,10k}/\mu_0$ .

X-ray diffraction measurement was carried out on the faces of the hexahedral cores parallel to the compacting direction, and the internal stress in the core was examined based on the integral breadth of the diffracted peak by  $\alpha$ -Fe (200).

## 3.2 Results

### 3.2.1 Initial permeability and integral width of green compacts

Table 2 shows  $\mu_{i,10k}/\mu_0$  of each sample and the integral breadth  $\beta$  of  $\alpha$ -Fe (200) in green compacts. Figures 2 and 3 show the relationship between green density and  $\mu_{i,10k}/\mu_0$  and that between  $\beta$  and  $\mu_{i,10k}/\mu_0$ , respectively, on the basis of the correlation shown in Fig. 1. Figure 2 shows the higher the compacting pressure (hence the packing fraction  $\eta$ ), the higher the value of  $\mu_{i,10k}/\mu_0$ . This result supports Eq. (1). Moreover, as shown in Fig. 3, it was found that the smaller the value of  $\beta$ , the higher the

32

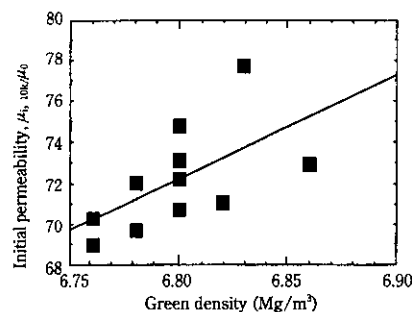


Fig. 2 Relation between green density and initial permeability at 10 kHz of iron powder cores

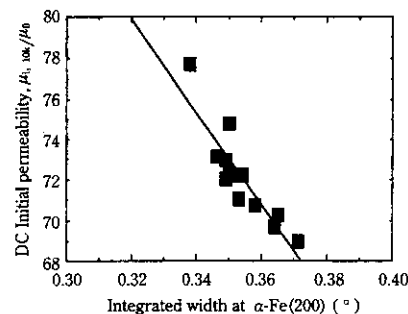


Fig. 3 Relation between integrated width on the surface of compacted body parallel to the compaction pressure and initial permeability at 10kHz of iron powder cores

value of  $\mu_{i,10k}/\mu_0$ .

### 3.2.2 Factors affecting green density

It has become apparent from an analysis of the compaction behavior of iron powder that the green density  $\rho$ , which shows the positive correlation to  $\mu_{i,10k}/\mu_0$ , depends on the surface shape of the particles and the hardness of the material<sup>9)</sup>. Hence, the relationship between  $\rho$  and the following parameters: the apparent density  $\rho_A$  ( $Mg/m^3$ ) reflecting the shape of particles, and the concentrations of impurities O, C, P and S,  $x_O$ ,  $x_C$ ,  $x_P$  and  $x_S$  (mass%) is found by multiple regression and the following equation is obtained:

$$\rho = 0.470\rho_A - 0.147x_O - 18.6x_C - 11.2x_P - 5.03x_S, \\ R^2 = 0.916 \dots\dots\dots (2)$$

It is apparent from Eq. (2) that the higher  $\rho_A$  and the lower the concentrations of impurities, the higher  $\rho$  will be. Because a powder with low  $\rho_A$  generally has great surface irregularities, the frictional resistance among particles is high, indicating that such powder is not easily closely packed by the rearrangement of particles during of pressure compacting. Further, it is concluded that plastic deformation does not occur easily due to solid solution hardening into a powder with high concentrations of impurities, especially C, P and S, which are solid-soluble elements, and due to precipitation harden-

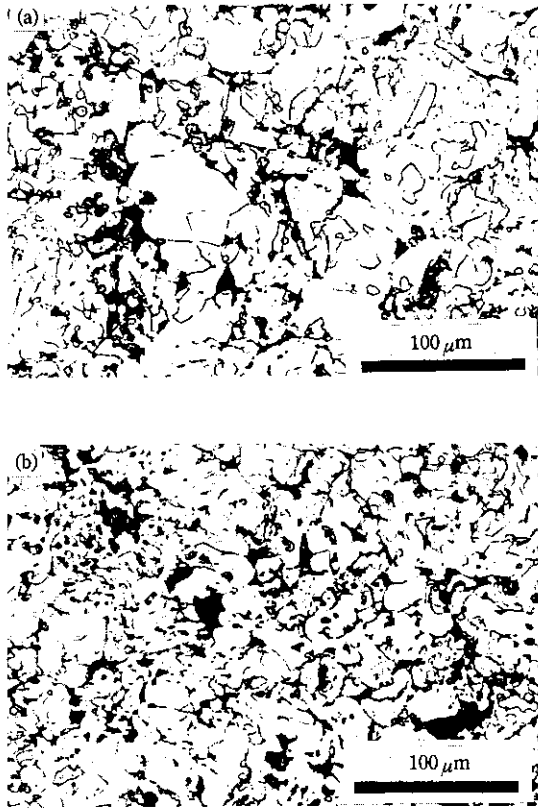


Photo 1 Optical micrographs of cross-section of reduced iron powder cores with  $\mu_{i,10k}/\mu_0$ : 75.9 (a) and 70.8 (b)

ing by the precipitation of carbides in a powder with a very high concentration of C, with the result that such powders are not easily closely packed.

### 3.2.3 Factors affecting $\beta$

As is apparent from Fig. 3,  $\beta$ , which has a strong negative correlation to  $\mu_{i,10k}/\mu_0$ , is related to the grain size  $\epsilon_0$  and strain  $\zeta$  by the following equation in the case of a metal which is worked<sup>10</sup>:

$$\beta \cos \theta/\lambda = 1/\epsilon_0 + 2\zeta \sin \theta/\lambda \dots \dots \dots (3)$$

where  $\theta$  denotes the diffraction angle of X-ray, and  $\lambda$  the wavelength of X-ray. From Eq. (3), the larger the grain size and the smaller the strain, the smaller  $\beta$  will be. Therefore, it is concluded from the results shown in Fig. 3 that  $\mu_{i,10k}/\mu_0$  is high in a core produced from iron powder of large grain size and small strain. It is known that strains provide barriers during domain wall displacement<sup>11</sup> and this fact is in agreement with this result. With respect to the relationship between grain size and  $\mu_{i,10k}/\mu_0$ , the structure was observed as shown below and an investigation was made into this relationship.

Photos 1 (a) and (b) show the optical micrographs of sections parallel to the compacting direction of green compacts at  $\mu_{i,10k}/\mu_0 = 75.9$  and 70.8, respectively.

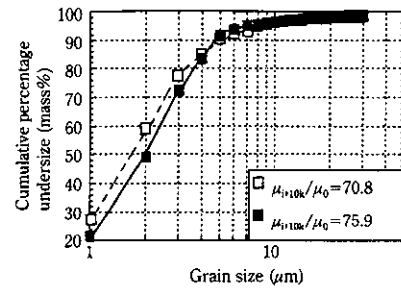


Fig. 4 Grain size distributions of  $\alpha$ -Fe in iron particles forming powder cores

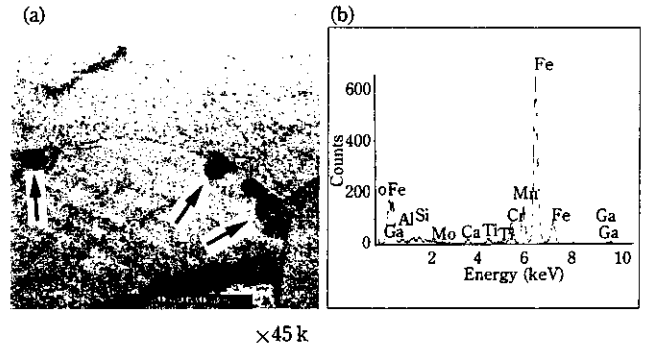


Fig. 5 TEM image around the grain boundary of the reduced iron powder (a) and EDX spectrum for the inclusion at the grain boundary observed in the TEM image (b)

In order to verify the quantitative relationship between grain size of  $\alpha$ -Fe and  $\mu_{i,10k}/\mu_0$ , the images of Photos 1 (a) and (b) were input into a computer and the grain sizes were evaluated. The grain size distribution (cumulative percentage undersize) is shown in Fig. 4. As is apparent from Fig. 4, the grain size of an iron powder in the core of low  $\mu_{i,10k}/\mu_0$  was larger than that of the iron powder in the core of high  $\mu_{i,10k}/\mu_0$ . It is considered that grain boundaries provide discontinuous surfaces of crystal structure and simultaneously act as the sites where dislocations introduced during plastic deformation accumulate and internal stresses are concentrated. Because this discontinuity of crystal structure and distribution of internal stresses forms extreme values of domain-wall energy, domain walls become less apt to move. Therefore, it might be thought that the grain boundaries in an iron powder core, whose iron powder is plastically deformed in the compacting process, function as barriers against the migration of magnetic fields.

The grain boundaries also provide sites of formation of precipitates. Figure 5 (a) shows a transmission electron microscope (TEM) image around the grain boundary in a thin layer of a reduced iron powder particle, which was prepared by using a focused ion beam (FIB). The width of the grain boundary was on the order of ten-odd nanometers and the existence of a second phase

was not observed with the exception of inclusions (the arrows in Fig. 5 (a)) 40 to 50 nm in diameter observed along the grain boundary. Figure 5 (b) shows an energy dispersed X-ray spectrum (EDS) of the precipitate observed in the grain boundary. Detected elements are Fe, O, Mn, Cr, Si, Ca, Ti, Al, Mo and Ga. Ga is considered to be derived from the radiation source of FIB and the inclusions at the grain boundaries are regarded as oxides including Fe, Mn, Cr, Si, Ca, Ti, Al and Mo. Most of these component elements are used in various kinds of steel materials and are considered to be the impurities derived from mill scale on the hot rolled steel, which is a raw material for reduced iron powder. Therefore, it is concluded that the observed inclusions remained at the grain boundaries in the reduction process of the scale powder. The thickness of a pure-iron domain wall has been estimated to be about 42 nm<sup>12)</sup>, which is almost the same size as a inclusion at the grain boundaries. When a nonmagnetic inclusion exists, the area of a domain wall decreases, resulting in a decrease in the domain-wall energy. In addition, the existence of a nonmagnetic inclusion reduces magnetostatic energy owing to the dimagnetic field generated by a magnetic pole occurring on the surface of the inclusion. As a result, the total energy of a magnetic material near the inclusion takes on a minimum value, thereby impeding the domain wall displacement. It is thought that, when the amount of inclusions is the same and the inclusions are distributed in a size almost the same as the thickness of the domain wall, the total energy reaches its minimum, with the result that inclusions function as strong pinning sites for the domain walls<sup>13)</sup>. Therefore, the grain boundaries in reduced iron particles contained in an iron powder core made are not only the sites of stress concentration but also the sites for nonmagnetic inclusions with a size almost the same as that of the thickness of the domain wall, serving as the pinning sites of the domain wall.

From the above results, it is concluded that the number of inclusions at and near the grain boundaries which impede the domain wall displacement is relatively small in an iron powder with a large grain size. Therefore, the density of pinning sites decreases, making the migration of the domain wall easy, and resulting in an increase in initial permeability.

#### 4 Features of High Permeability Reduced Iron Powder KIP MG270H

##### 4.1 Initial Permeability

A high-permeability reduced iron powder for line filter cores, KIP MG270H, was developed by lowering the concentrations of impurities O, C, P and S, improving compressibility, and increasing the size of grains on the basis of the knowledge obtained in the present study. Table 3 shows the typical specifications of KIP

Table 3 Typical values of characteristics of iron powders

	MG270H	270MS
Chemical composition (mass%)		
Total Fe	99.4	99.4
Total C	0.001	0.003
Si	0.03	0.03
Mn	0.24	0.24
P	0.010	0.013
S	0.003	0.005
Apparent density (Mg/m <sup>3</sup> )	2.70	2.66
Particle size distribution (mass%)		
+ 48 mesh	n.d.	n.d.
+ 100 mesh	1.2	1.9
+ 150 mesh	21.0	22.5
+ 200 mesh	33.8	32.0
+ 250 mesh	11.0	10.0
+ 325 mesh	18.7	18.2
- 325 mesh	14.3	16.0
Green density (Mg/m <sup>3</sup> )	6.84	6.80
Initial permeability	76	71

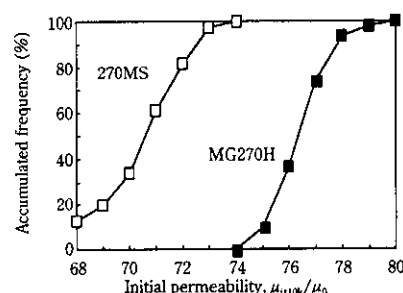


Fig. 6 Accumulated frequency of initial permeability of iron powder cores

MG270H and the conventional magnetic material KIP MG270MS and Fig. 6 shows the accumulated frequency percentage of the value of  $\mu_{i,10k}/\mu_0$  of 60 lots of both products. In KIP MG270H, the concentrations of impurity elements are lower than in the conventional material and the apparent density and green density are higher, with the result that  $\mu_{i,10k}/\mu_0$  is improved. Moreover, as is apparent from Fig. 6, the dispersion of  $\mu_{i,10k}/\mu_0$  is decreased to half, therefore, KIP MG270H has better characteristics.

##### 4.2 Iron Loss

The purpose of this study is to improve the initial permeability of reduced iron powder. However, the results of an investigation of the iron loss of iron powder cores made of the developed material are given below for reference.

###### 4.2.1 Experimental methodology

Iron losses were measured in the developed mater-

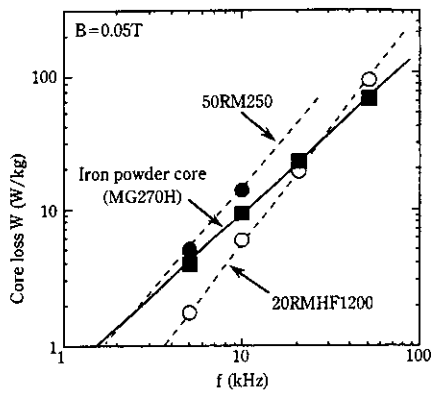


Fig. 7 Core losses of the iron powder core and electrical steels

ial KIP MG270H and the non-oriented magnetic steel strips 50RM250 (0.5 mm thick, JIS conforming material) and 20RMHF1200 (0.2 mm thick, high-frequency-compatible material) made by Kawasaki Steel as comparative materials.

KIP MG270H was mixed with 2 mass% epoxy resin and the mixture was formed at 686 MPa into a ring 38 mm in outer diameter, 25 mm in inner diameter and 6.2 mm in height. After that, an iron core was obtained by thermosetting the resin at 553 K for 30 min. As for the non-oriented magnetic steel strips, test pieces in ring form with a size of 30 mm in outer diameter and 20 mm in inner diameter were obtained by electrical discharge machining. Iron losses were measured by means of a BH-analyzer (type E5060A made by Hewlett-Packard Japan, Ltd.) under the conditions of a maximum flux density of 0.05 T and frequencies of 1 kHz to 100 kHz.

#### 4.2.2 Results of the experiment

The frequency dependence of the iron loss of each sample is shown in Fig. 7. Iron losses of KIP MG270H are lower than those of 50RM250 at not less than 2.5 kHz and further lower than those of 20RMHF1200 at not less than 25 kHz. This indicates that iron powder cores of KIP MG270H should be used in the frequency band of 1 kHz to hundreds of kilohertz, which is in the gap between the frequency bands where magnetic steel strip cores and sintered ferrite cores are independently used.

## 5 Conclusions

Factors affecting the initial permeability of reduced

iron powder for noise filters were analyzed and a high-permeability reduced iron powder for noise filters, KIP MG270H, was developed on the basis of obtained knowledge as follows.

- (1) The green density was increased by lowering the concentrations of O, C, P and S or increasing the apparent density of powder. It is possible to improve the initial permeability of an iron powder core by increasing the green density.
  - (2) The smaller the strain in an iron powder core and the larger the grain size, the higher the initial permeability.
  - (3) It was ascertained that nonmagnetic inclusions of almost the same size as the width of the domain wall were present at the grain boundaries. This suggests that the grain boundaries acted as effective pinning sites. It is possible to improve the initial permeability of an iron powder core by increasing the size of grain.
- Iron losses of an iron powder core made of KIP MG270H are low in the frequency band of 1 kHz to hundreds of kilohertz, which is in the gap between the frequency bands where magnetic steel strip cores and sintered ferrite cores are independently used. The application of iron powder cores made of KIP MG270H in this frequency band is expected.

## References

- 1) K. Fukui, I. Watanabe, and M. Morita: *IEEE Trans. Magn.*, MAG-8(1972), 682
- 2) K. Fukui, T. Oshima, and S. Watanabe: *Toshiba Review*, 28 (1973), 238
- 3) T. Nishida, T. Kikuchi, T. Sato, and T. Ichiyama: *J. of Jpn. Inst. of Metals*, 42(1978)6, 593
- 4) T. Nishida, S. Mizoguchi, M. Yamamiya, T. Hashizume, and Y. Nakamura: *J. of Jpn. Inst. of Metals*, 42(1978)6, 600
- 5) C. H. Sellers, T. A. Hyde, and D. E. Gay: Proc. 1996 World Congr. Powder Metallurgy and Particulate Materials, (1996), 20-99
- 6) F. Ollendorf: *Arch. Elektrotechn.*, 25(1931), 436
- 7) S. Takajo: "Study on Analysis of Magnetic Properties Manufacture of Iron Powder and Sintered Core Materials," Univ. of Tohoku, (1987), 14, doctoral dissertation
- 8) S. Takajo and Y. Kiyota: *J. of Jpn. Soc. of Powder*, 32(1985)7, 259
- 9) Y. Ozaki, K. Ogura, and M. Kawaguchi: Abstracts of Spaing Meeting of J. Soc. of Powder, (1998), 92
- 10) W. Hall: *Proc. Phys. Soc.*, A62(1949), 741; *J. Inst. Met.*, 75(1950), 1127
- 11) J. L. Snoek: "New Developments in Ferromagnetic Materials", (1949), §17, 54, [Elsevier, Amsterdam]
- 12) S. Chikazumi: "Physics of Ferromagnetic Materials (Vol. 2) (3rd edition)", (1987), 174, [Shokabo]
- 13) L. Neel: *J. Phys. Rad.*, 9(1948), 184